Defect engineered Z-scheme polymeric C_3N_4/CdS heterojunction mediated by Ag boosting dual-channel H_2O_2 production with synergistic antibiotic degradation

YongJian Sun[a], Xiangdong Wang[a], Hui Liu[a], Xintao Feng[a], Andre Lennox Olayemi Macauley[a], Wenli Zhang[a], Yinhua Jiang[a,*], Yan Liu[a] , Jianming Zhang[a] , Haiqing Xu[b,*]

a. School of Chemistry and Chemical Engineering, Jiangsu University, Zhenjiang 212013, P. R. China.

b. National & Local Joint Engineering Research Center for Deep Utilization Technology of Rock-salt Resource, Faculty of Chemical Engineering, Huaiyin Institute of Technology, Huaian 223003, P. R. China.

Corresponding authors: E-mail address: *jyhua@ujs.edu.cn (Y.H. Jiang), *xuhaiqing@hyit.edu.cn (H.Q. Xu), ; Fax: +86 511 88791800; Tel.: +86 511 8879 0187.

Chemicals and materials

Urea (CH_3N_2O), Silver nitrate ($Ag(NO_3)$), cadmium acetate dihydrate ($(CH_3COO)_2Cd{\cdot}2H_2O$), Sodium sulfide nonahydrate ($Na_2S{\cdot}9H_2O$), sodium hydroxide (NaOH), Potassium Hydrogen Phthalate ($C_8H_5O_4K$), potassium iodide (KI), ammonium molybdate ($(NH_4)_2MoO_4$), sodium sulfate (Na_2SO_4), potassium ferricyanide ($K_3Fe(CN)_6$), potassium chloride (KCl), potassiun ferrocyanide ($K_4Fe(CN)_6$), 1,4-Benzoquinone ($C_6H_4O_2$), isopropanol (C_3H_8O) and phenol (C_6H_6O). All the chemical reagents used in the experiment were of analytical grade without further purification.

Photocatalytic performance testing

The photocatalytic activity of the materials used to degrade AMX while producing hydrogen peroxide was evaluated at room temperature (20 ℃) and pressure. A 300 W xenon lamp (Microsolar300, Beijing Perfect-light) equipped with a visible-light cutoff filter ($\lambda > 420$ nm) was used as the irradiation source, with an average light intensity of 123.46 $mW{\bullet}cm^{-2}$. The prepared photocatalyst (20 mg) was dispersed into 60 mL solution (51 mL deionized water plus 9 mL 100 mg/L AMX solution) in a quartz container. To ensure adsorption equilibrium in the photocatalytic experiments, the solution was stirred in the dark for 30 min before irradiation. 4 mL reaction liquids were obtained at every 20 mins after light was on, which was filtered using a 0.45 μM PTFE syringe filter (Millex) for further analysis of H_2O_2 content and AMX degradation efficiency by UV-visible spectroscopy. In addition, the experiment for H_2O_2 production in pure water was carried out using the above similar process only by replacing 60 mL

of AMX solution with 50 mL of deionized water.

Measurement of H_2O_2 concentration

The concentration of H_2O_2 was determined by iodine titration [1]. Take 1 mL sample and add 0.25ml 0.1 mol/L $C_8H_5O_4K$ and 0.25 mL KI mixture (0.4 mol/L KI + 0.06 mol/L NaOH + 0.0001 mol/L $(NH_4)_2MoO_4$). After waiting for 20 min for the color development to be completed, take 1 mL of the color development solution and diluted 10 times, the hydrogen peroxide content was evaluated by a UV-visible spectrophotometer (Shimadzu UV UV/Vis 2450, Japan). The reaction mechanism is as follows:

$$H_2O_2 + 3I^- + 2H^+ \rightarrow I_3^- + 2H_2O$$

The concentration of H_2O_2 was calculated by the concentration formula (y=1776.205x). I_3^- peaks at around 352 nm in the UV-vis spectrum.

Measurement of the degree of AMX degradation

2 ml sample was used to evaluate the degree of degradation by a UV-vis spectrophotometer (Shimadzu UV UV /Vis 2450, Japan). AMX has a peak at about 228 nm in the UV-visible spectrum [2]. The degree of AMX degradation was assessed using the following formula:

$$Q = \frac{C_0 - C}{C_0} \times 100\%$$

Where, Q is the degree of AMX degradation, C_0 represents the absorbance of the initial sample and C represents the absorbance of the current sample.

The Materials characterization:

PCN, Ag-PCN, CdS, Vs-CdS and Ag-PCN/Vs-CdS composites were subjected to phase structure and crystallinity measurements using an X-ray diffractometer (XRD, Rigaku Rotaflex D/MAX-2500) equipped with Cu Kα radiation (λ = 1.54178 Å) that scanned between 10 and 80° at a rate of 5° min^{-1}. Scanning electron microscopy (SEM, JSM-7800F) and transmission electron microscopy (TEM, JEM-2100) were used to examine the morphology and structure of the resultant samples. A dispersive x-ray spectrometer analyzer (EDS) was connected to a high-resolution transmission electron microscope (HR-TEM; FEI Tecnai G2 F20 S-TWIN) for the purposes of lattice fringing, elemental distribution studies, and selected area electron diffraction (SAED). The materials' composition and chemical state were investigated using Thermal Sciences' ESCALAB 250Xi x-ray photoelectron spectrometer (XPS). The Micromeritics ASAP2020 instrument and the Brunauer-Emmett-Taylor (BET) equation were used to determine the specific surface area and aperture distribution. The Zeta potential of the photocatalysts was measured on a NanoBrook 90plus Pals Zeta Potential and Particle Size Analyzer at room temperature, using aqueous suspensions after sonication for 20 min, and the average values were obtained from three independent measurements. The contact angle was determined on a KSV, CAM 200 using the sessile drop method with deionized water as the probe liquid, and each reported value represents the average of three measurements at different positions on the sample surface. Using barium sulfate as a standard reflecting material, the UV-Vis diffuse reflectance spectra were recorded using a UV-Vis spectrophotometer (UV-

2450, Shimadzu) in order to investigate the optical characteristics and determine the band gap of the photocatalytic material. The Photoluminescence (PL) spectra were investigated by PerkinElmer LS 55 spectrophotometer. The photocurrent response, EIS and Mott-Schottky plots were tested with a standard three-electrode system.

Photoelectrochemical performance testing:

An electrochemical workstation from Chenhua, Shanghai, model number CHI660E was used for the electrochemical investigations. Using 0.5 M Na_2SO_4 solution as the electrolyte, a 300 W xenon lamp ($\lambda > 420$ nm) as the light source, and Pt sheet and Ag/AgCl electrodes as pair electrode and reference electrode, respectively, the transient photocurrents of the photocatalysts were investigated. To produce the working electrodes, 5 mg of photocatalyst was ultrasonically dispersed in 1 mL of ethylene glycol solution. The suspension was then dropped onto a conductive glass (1.0*1.0 cm^2) that had been insulated with epoxy glue and dried at 60 °C for a whole night. Mott-Schottky plots were obtained without the use of a light source. When the electrolyte was a mixture of 0.5 M KCl/5 mM $K_3[Fe(CN)_6]$/5 mM $K_4[Fe(CN)_6]$, the electrochemical impedance spectroscopy (EIS) curve was measured.

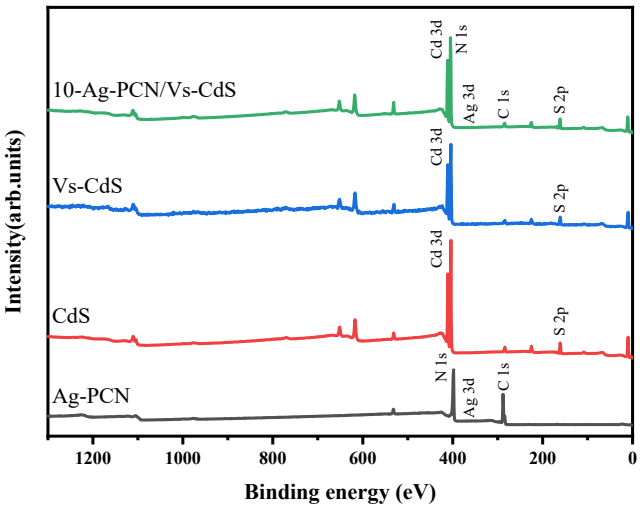

Fig. S1 XPS survey spectrum.

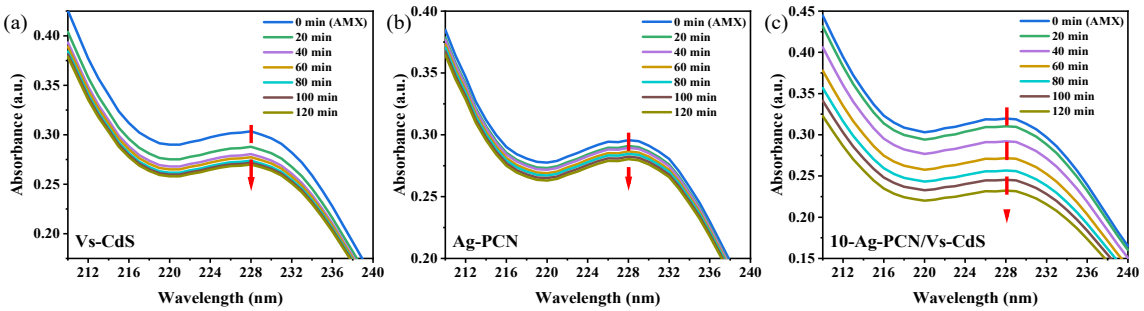

Fig. S2 Time-dependent UV–Vis absorption spectra of amoxicillin (AMX) aqueous solution during photocatalytic degradation of (a) Vs–CdS, (b) Ag–PCN, and (c) 10Ag–PCN/Vs–CdS.

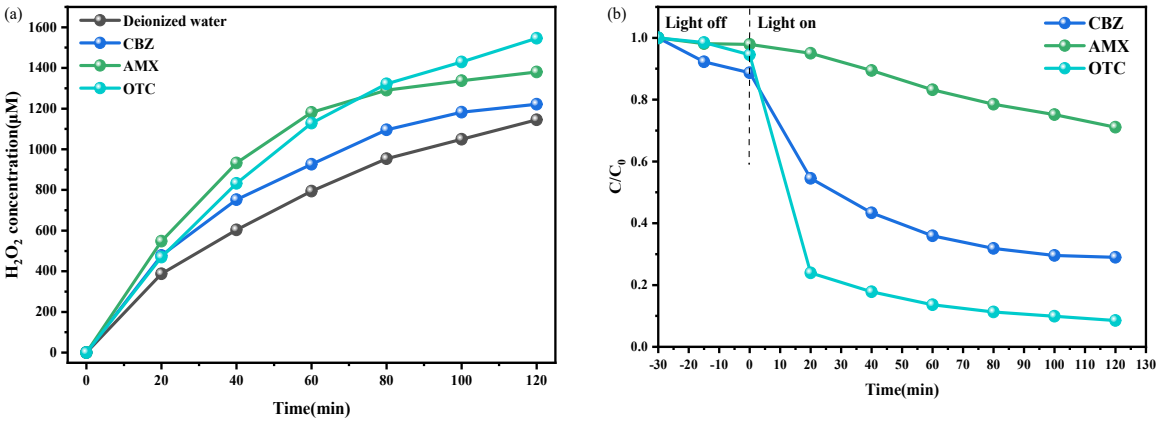

Fig. S3 (a) Photocatalytic generation of H_2O_2 while degrading 15 mg/L different pollutants with 10-Ag-PCN/Vs-CdS and (b) photodegradation curves of different pollutants under visible light irradiation ($\lambda > 420$ nm).

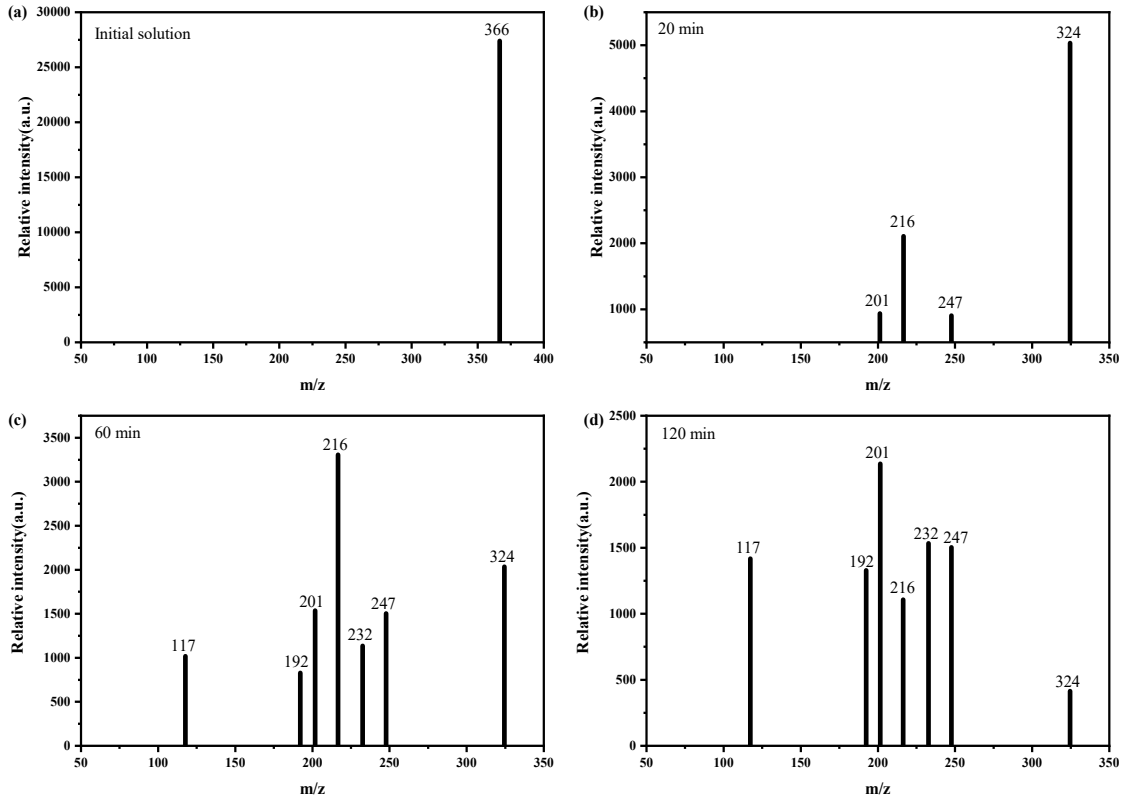

Fig. S4 (a-d) Typical MS of photodegradation products obtained by UHPLC-MS method.

Table S1 Preparation of H_2O_2 with simultaneous degradation of organic pollutants by 10Ag-PCN/Vs-CdS and other recently reported photocatalysts.

Photocatalyst	**Light source**	**Reaction solution**	**[H_2O_2]/μmol g^{-1} h^{-1}**	**Ref.**
Cl-$ZnIn_2S_4$/TpPa-1	λ > 400 nm	TCH	846	[3]
Ti_3C_2/SA-TCPP	λ > 400 nm	2,4-DCP	247.3	[4]
TiO_2/$BiOBr_{0.5}Cl_{0.5}$	simulated sunlight	TCH	133.9	[5]
K, P, O-CN_X	λ > 420 nm	OXC	92.9	[6]
NC-x	λ > 420 nm	DCF	920	[7]
TiO2/COF	simulated sunlight	RhB	1326	[8]
PCCN	λ > 420 nm	BPA	374.4	[9]
HTNIMS	simulated sunlight	CIP	165.5	[10]
10-Ag-PCN/Vs-CdS	**λ > 420 nm**	**AMX**	**1725.3**	**This work**

References

1. O. Tomita, T. Otsubo, M. Higashi, B. Ohtani and R. Abe, *ACS Catal*, 2016, **6**, 1134-1144.
2. M. Moslemi-Eilanlou, A. Habibi-Yangjeh, Z. Salmanzadeh-Jamadi and A. Khataee, *J. Alloys Compd*, 2025, **1031**, 180936.
3. G. Xia, J. Qiu, D. Dai, Y. Tang, Z. Wu and J. Yao, *Catal. Sci. Technol.*, 2024, **14**, 590-597.
4. Q. Wang, X. Lu, S. Qi, X. Yu, P. Liang, X. Han, Z. Wang and J. Yang, *Sep. Purif. Technol*, 2025, **361**, 131363.
5. K. Chai, X. Feng, L. Li, M. Kuai, J. Xu, Z. Ni, P. Zhang and W. Xu, *Appl. Surf. Sci*, 2025, **710**, 163976.
6. D. Chen, B. Yao, X. Zhi, C. Tian, M. Chen, S. Cao, X. Feng, H. Che, K. Zhang and Y. Ao, *Nanoscale*, 2023, **15**, 11482-11490.
7. Z. Guo, C. Zhao, L. Meng, H. Fu, C. Wang, Z. Chen, Y. Zheng, Y.-H. Li, J.-F. Wang and C.-C. Wang, *Appl. Catal. B Environ*, 2025, **377**, 125507.
8. Y. Zhao, Y. Zhang, H. Tan, C. Ai and J. Zhang, *J. Materiomics*, 2025, **11**, 100970.
9. T. Li, X. Zhang, C. Hu, X. Li, P. Zhang and Z. Chen, *J. Environ. Chem. Eng*, 2022, **10**, 107116.
10. B. Li, C. Ning, Y. Pan, X. Li, X. Wang and Z. Chen, *J. Environ. Chem. Eng*, 2025, **13**, 115301.